Article

The TaCLE24b peptide signaling cascade modulates lateral root development and drought tolerance in wheat

Wen Yang[1,4], Man Feng[1,4], Kuohai Yu[1], Jie Cao[1], Guangxian Cui[1], Yumei Zhang[2], Huiru Peng[1], Yingyin Yao[1], Zhaorong Hu[1], Zhongfu Ni[1], Feng Qin[1], Fuminori Takahashi[3], Qixin Sun[1] & Mingming Xin[1] ✉

Plant peptide hormones play an important role in regulating root development and stress responses. Here, we identify a root-derived CLAVATA3/Endosperm surrounding region-related (CLE) peptide TaCLE24b and its leucine-rich repeat receptor-like kinase CLAVATA1 (CLV1) TaCLV1, which together regulate the formation of lateral root primordium and the outgrowth of lateral root in wheat. Additionally, a loss-of-function mutation of *TaSG-D1*, encoding a Ser/Thr protein kinase glycogen synthase kinase 3 (STKc_GSK3), also enhances the formation of lateral root primordium and the outgrowth of lateral roots in wheat. Furthermore, TaCLV1 interacts with TaSG-D1, leading to phosphorylation and degradation of TaSG-D1. Whereas the presence of TaCLE24b enhances the binding affinity and phosphorylation ability of TaCLV1 to TaSG-D1, thereby positively fine-tuning lateral root development and contributing to drought tolerance in wheat. Overall, our findings provide new insights into the significance of the peptide signaling pathway in regulating lateral root development and responding to drought stress in wheat.

Lateral roots constitute a vital element of root architecture, exerting a significant influence on plant growth and development. They serve as key conduits for water and nutrient uptake, substantially augmenting the surface area of the actively absorbing root system, which is closely associated with the response to water deficit[1]. Wheat (*Triticum aestivum* L.) is a critically important crop that provides calorific intake for ~35% of the global population[2]. However, wheat is highly vulnerable to drought stress, resulting in significant yield losses in conditions of drought stress[3]. Therefore, identifying new genes and developing effective strategies to enhance drought tolerance in wheat are essential for the next green revolution.

Plant secreted peptides, translated from small open reading frames (sORF <100 amino acids [aa]), have been demonstrated to trigger intercellular communications to regulate diverse processes in plants via interacting with their cognate kinase receptors[4–6], including

the regulation of lateral root emergence and formation[7–13]. For example, the TARGET OF LBD SIXTEEN 2 (TOLS2) peptide inhibits lateral root initiation together with RECEPTOR-LIKE KINASE7 (RLK7) in Arabidopsis (*Arabidopsis thaliana*) through upregulation of transcription factor *PUCHI*, and loss of *TOLS2-RLK7* signaling increases lateral root number[14]. CLAVATA3/EMBRYO-SURROUNDING REGION-related peptides (CLE) genes are also involved in the regulation of lateral root development, and simultaneous loss-function of *CLE16* and *CLE17* leads to prolonged transition phase of lateral root development, eventually resulting in a reduction in the number of emerged lateral roots[13]. In addition, The TRACHEARY ELEMENT DIFFERENTIATION INHIBITORY FACTOR (TDIF) binds to the TDIF receptor (TDR), and triggers the activation of BRASSINOSTEROID-INSENSITIVE2 (BIN2), which then phosphorylates AUXIN RESPONSE FACTOR7 (ARF7) and ARF19, inhibiting their interactions with repressor proteins associated

[1]Frontiers scientific center for molecular design breeding, China Agricultural University, Beijing 100193, China. [2]Qingdao Agricultural University, Qingdao 266109, China. [3]Faculty of Advanced Engineering, Tokyo University of Science, Tokyo 125-8585, Japan. [4]These authors contributed equally: Wen Yang, Man Feng. ✉ e-mail: mingmingxin@cau.edu.cn

with AUXIN/INDOLE-3-ACETIC ACID (AUX/IAA), and positively regulates lateral root development in Arabidopsis[9]. Moreover, plant peptides also play important roles in response to environmental stresses. When facing drought stress, CLE25 serves as a messenger, conveying signals of water deficiency from roots to leaves via the vascular tissue. Upon reaching the leaves, CLE25 interacts with and activates BAM1 and BAM3 receptor, which, in turn, leads to the modulation of ABA accumulation and subsequent stomatal closure[6]. The wheat genome contains >30,000 sORFs with unknown functions (IWGSCv1.1) and the contribution of these genes to wheat development and stress responses remains largely unknown.

In this work, we identify a root-derived peptide TaCLE24b, which binds to the leucine-rich repeat receptor-like kinase TaCLV1 and contributes to lateral development. The TaCLV1 interacts with and phosphorylates TaSG-D1, leading to its degradation. Whereas the presence of TaCLE24b enhances the binding affinity and phosphorylation ability of TaCLV1 to TaSG-D1, thereby positively fine-tuning lateral root development and consequently drought strss tolerance in wheat.

Results

TaCLE24b positively regulates lateral root development in wheat

Previous study has predicted 104 CLE genes in wheat genome, and nearly half of which exhibited higher transcript abundance in wheat roots than in other tissues according to the published transcriptome data[15], indicating their potential roles in the regulation of root development. Of these, TraesCS5B02G418500 (hereafter designed as *TaCLE24b* according to the previous study[15]) was mainly expressed in seedling root according to RT-qPCR analysis, whereas its homeologs of *TaCLE24a* and *TaCLE24d* are barely expressed in all examined tissues (Fig. 1a and Supplementary Fig. 1a). Therefore, we selected *TaCLE24b* as the candidate for further analysis. Further β-Glucuronidase (GUS) reporter-aided histochemical analysis demonstrated that the *TaCLE24b* promoter is predominantly active in the lateral root primordia and root tips of wheat (Fig. 1b), which was further confirmed by in situ hybridization (Supplementary Fig. 1b).

To investigate the biological significance of wheat *TaCLE24b*, we chemically synthesized its encoded peptide (RLSPGGSNPQHH), and applied exogenously 0.1 μM TaCLE24b to the root of wheat seedlings. We meticulously assessed the effects of TaCLE24b treatment on the formation of lateral root primordium (LRP) and the outgrowth of lateral root (LR) along the primary root of 9 day-old seedlings. LRP situated in the LR formation zone was categorized as "developing LRP (DLRP)". LR positioned in the root branching zone was designated as "emerged LR (ELR)". LRP located in the branching zone of the root that have not yet breached the epidermis was referred to "Non-emerged LRP (NELRP)"[16] (Fig. 1c). We observed that the density of DLRP and ELR were notably higher in the experimental group (0.1 μM TaCLE24b) compared to the control group (0 μM TaCLE24b), while the density of NELRP showed no significant differences between each other (Fig. 1d, e). In addition, we generated *TaCLE24b* overexpression lines in the wheat cultivar CB037 background by using the constitutively active *Ubiquitin* promoter to drive the target gene. Transgenic lines (*TaCLE24bOE-2* and *TaCLE24b-OE-3*) showed phenotypes similar to exogenous application of TaCLE24b, with ~61.8% and 60.3% increases of ELR density, respectively, compared to the wild type (WT, average of 0.542 and 0.537 vs. 0.335 for WT [CB037]), and with ~73.6% and 88.8% increases of DLRP density, respectively, compared to the wild type (average of 0.571 and 0.621 vs. 0.329 for WT [CB037]; Fig. 1f). Furthermore, CRISPR/Cas9-mediated gene editing was explored to simultaneously knock out the three homeologs of *TaCLE24* in the wheat cultivar Fielder background. The *TaCLE24* triple knockout mutants *Tacle24cr-3* and *Tacle24cr-6* exhibited ~19.2% and ~22.5% decreases of ELR density, respectively, compared to the WT (average of 0.699 and 0.670 vs. 0.865 for WT [Fielder]), as well as -22.6% and

~22.8% decreases of DLRP density, respectively, compared to the WT (average of 0.580 and 0.578 vs. 0.749 for WT [Fielder]; Fig. 1g and Supplementary Fig. 2a). Furthermore, the formation of lateral root primordium and the outgrowth of lateral root of the *TaCLE24* loss-of-function mutant lines were comparable to the WT following exogenous TaCLE24b peptide application (Fig. 1h). These lines of evidence suggest that *TaCLE24b* positively regulates lateral root primordium formation and lateral root outgrowth in wheat.

TaCLE24b-induced promotion of lateral root development requires TaCLV1

Peptide hormones are often recognized by corresponding receptors, which then transmit signals to downstream targets to fine-tune plant growth or stress responses[17–19]. To identify potential candidate receptors involved in the TaCLE24b peptide signaling pathway in wheat, we screened a subset of leucine-rich repeat receptor-like kinases (Methods, Supplementary Fig. 2b), and selected TraesCS7D02G521200 (designed as *TaCLV1*), a homolog of Arabidopsis *CLV1*, for subsequent analysis. *TaCLV1* exhibited a similar expression pattern to *TaCLE24b*, and was mainly expressed in lateral root primordium and root tip based on RT-qPCR and in situ hybridization (Fig. 2a, b and Supplementary Fig. 2c). The TaCLV1 protein localized to the plasma membrane, as shown by transient expression analysis in *Nicotiana benthamiana* leaves (Supplementary Fig. 2d). We then demonstrated that mature TaCLE24b peptide interacted with leucine-rich repeat (LRR) domain of TaCLV1 via microscale thermophoresis (MST) assay and obtained the calculation of the dissociation constant (K_d value) of 19.35 ± 5.03 nM (Fig. 2c).

To identify biological importance of *TaCLV1*, we attempted to knock out all three *TaCLV1* homeologs simultaneously using CRISPR/Cas9 editing strategy, however, we were unable to generate homozygous mutant lines with knockout of all A-, B-, and D-homeologs, likely due to the lethality associated with the complete loss of *TaCLV1* function. Therefore, we identified knockout lines with homozygous mutation of two *TaCLV1* homeologs, while leaving the last one heterozygous (designed as *Taclv1cr-12* and *Taclv1cr-15*; *Taclv1cr-12*: homozygous mutations in the A- and B- genomes, and heterozygous mutation in the D- genome; *Taclv1cr-15*: homozygous mutations in the A- and D- genomes, and heterozygous mutation in the B- genome; Supplementary Fig. 2e). Nonetheless, the two *TaCLV1* mutant lines exhibited a significant reduction in lateral roots, with almost 39.1% and 44.1% decreases of ELR density, respectively, compared to the WT (average of 0.557 and 0.511 vs. 0.914 for WT [Fielder]), as well as -52.3% and ~44.1% decreases of DLRP density, respectively, compared to the WT (average of 0.405 and 0.475 vs. 0.849 for WT [Fielder], Fig. 2d). Furthermore, although the heterozygous *TaCLV1* mutants still exhibited responses to TaCLE24b peptide treatment in terms of lateral root primordium formation and lateral root outgrowth, their sensitivity to TaCLE24b peptide is evidently diminished compared to WT (Fig. 1e and Fig. 2e), supporting the notion that TaCLV1 is the cognate receptor of TaCLE24b with dosage effects, and is required for the TaCLE24b-mediated signaling module in the promotion of lateral root development in wheat.

The TaCLE24b-TaCLV1 signaling pathway interacts with TaSG-D1 to modulate lateral root development

We previously conducted map-based cloning of *TaSG-D1* (TraesCS3D02G137200) gene, a homolog of Arabidopsis *BRASSINOSTEROID-INSENSITIVE2* (*BIN2*). It was discovered that a single amino acid substitution (E286K) of TaSG-D1 (referred to as TaSG-D1^{E286K}) results in semispherical grain phenotype in *Triticum sphaerococcum*[20], and increases protein stability under normal conditions or in response to heat stress[21]. Here, we compared the lateral root development of near-isogenic lines that differed at the *TaSG-D1^{E286K}* (designated as NIL-K) or *TaSG-D1* (designated as NIL-E) locus,

and observed that the NIL-K lines exhibited a significant reduction of density of ELR and DLRP compared with NIL-E (average of 0.773 [NIL-K] vs. 1.396 [NIL-E] for ELR, and average of 1.244 [NIL-K] vs. 1.672 [NIL-E] for DLRP, ND4332 background; Fig. 3a, b). In addition, we found that EMS-induced loss-of-function mutation of $TaSG\text{-}D1^{E286K}$ (designated as M2-1) increases the density of ELR and DLRP by 111.6% and 56.8% compared to the WT (average of 1.697 [M2-1] vs. 0.802 [ND4332] for ELR, average of 1.634 [M2-1] vs. 1.042 [ND4332] for

DLRP, ND4332 background, Fig. 3a and Supplementary Fig. 3a). Similarly, the E286K substitution in the $TaSG\text{-}D1$ homeolog (TraesC-S3A02G136500, located on chromosome 3A, designated as A236) also led to reduced density of ELR and DLRP compared to the WT (average of 1.130 [A236] vs. 1.638 [NC4] for ELR, average of 0.846 [A236] vs. 1.204 [NC4] for DLRP, NC4 background, Fig. 3a and Supplementary Fig. 3b). Additionally, we investigated the lateral root development of NIL-K and NIL-E in response to TaCLE24b peptide
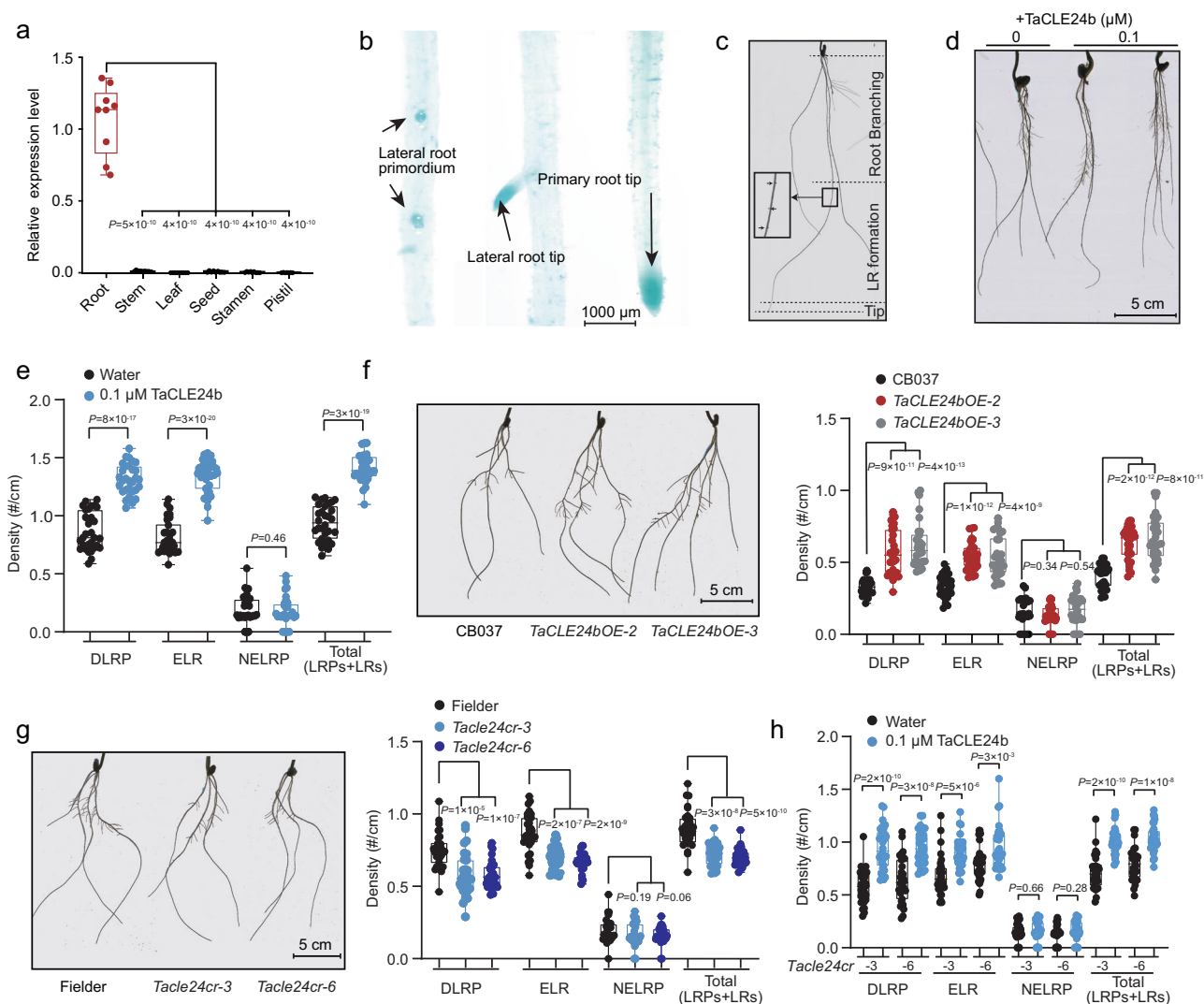

Fig. 1 | TaCLE24b positively contributes to lateral root development in wheat.
a RT-qPCR analysis shows the root-specific expression of *TaCLE24b* in wheat. The mean expression level of *TaCLE24b* in roots is set to 1.00. The box plots display the interquartile range, comprising the first quartile, median, and third quartile, while the whiskers extend from the minimum to the maximum values. Two-tailed Student's *t*-test, (*n* = 9). **b** GUS staining shows the expression patterns of *TaCLE24b* in the lateral root tip, primary root tip, and lateral root primordium of wheat (*n* = 3). Scale bar, 1 mm. **c** Schematic analysis of three developmental zones of primary root regarding lateral root formation and outgrowth in wheat. The arrows indicate the magnified view of this region. **d** Phenotypic analysis of wheat seedlings in response to exogenous application of synthesized TaCLE24b. Fielder wheat seedlings were subjected to 9 day treatment with TaCLE24b at the 0.1 μM concentration before phenotyping. Scale bar, 5 cm. **e** Statistical analysis of wheat seedlings in response to exogenous application of 0.1 μM synthesized TaCLE24b. The box plots display the interquartile range, comprising the first quartile, median, and third quartile, while the whiskers extend from the minimum to the maximum values. Two-tailed Student's *t*-test, (*n* = 30). DLRP: developing LRP; ELR: emerged LR; NELRP: non-emerged LRP. **f** Overexpressing *TaCLE24b* results in increased density of lateral

root and lateral root primordium in CB037. Scale bar, 5 cm. Phenotyping was performed using 9 day-old seedlings of *TaCLE24b* overexpression lines (*TaCLE24bOE-2* and *TaCLE24bOE-3*) and wild type (CB037) cultured in Hoagland medium. The box plots display the interquartile range, comprising the first quartile, median, and third quartile, while the whiskers extend from the minimum to the maximum values. Two-tailed Student's *t*-test, (*n* = 30). **g** *TaCLE24* knockout mutants show decreased density of lateral root and lateral root primordium compared to the control. Scale bar, 5 cm. Phenotyping was performed using 9 day-old seedlings of *TaCLE24* knockout lines (*Tacle24cr-3* and *Tacle24cr-6*) and wild type (Fielder) cultured in Hoagland medium. The box plots display the interquartile range, comprising the first quartile, median, and third quartile, while the whiskers extend from the minimum to the maximum values. Two-tailed Student's *t*-test, (*n* = 30). **h** Comparison of lateral root density and lateral root primordium density of 9 day-old seedlings between *Tacle24* knockout mutants (*Tacle24cr-3* and *Tacle24cr-6*) and wild type (Fielder) in response to TaCLE24b peptide application. The box plots display the interquartile range, comprising the first quartile, median, and third quartile, while the whiskers extend from the minimum to the maximum values. Two-tailed Student's *t*-test, (*n* = 30).

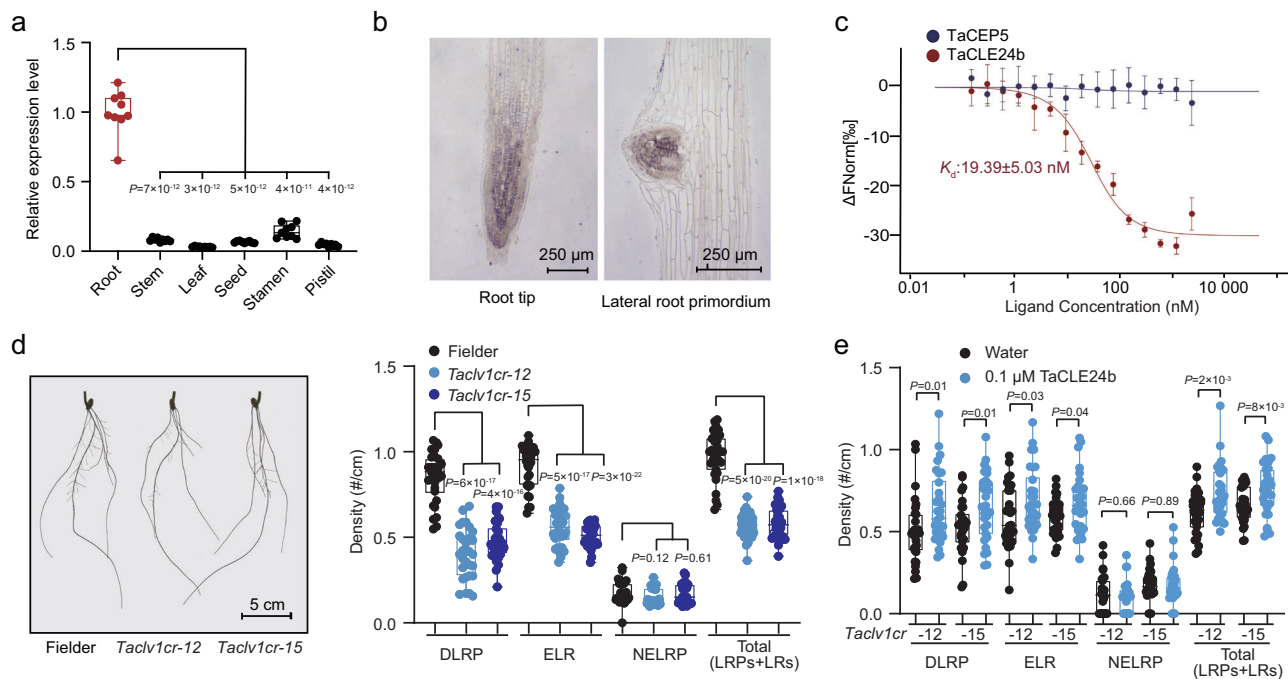**Fig. 2 | Receptor-like kinase TaCLV1 regulates lateral root development via interacting with the TaCLE24b peptide. a** RT-qPCR analysis shows the root-specific expression of *TaCLV1* in wheat. The mean expression level of *TaCLV1* in roots is set to 1.00. The box plots display the interquartile range, comprising the first quartile, median, and third quartile, while the whiskers extend from the minimum to the maximum values. Two-tailed Student's *t*-test, ($n = 9$). **b** In situ hybridization shows the tissue-specific expression of *TaCLV1* in root tip and primordium ($n = 3$). Scale bars, 250 µm. **c** Microscale thermophoresis (MST) analysis shows the physical interaction between TaCLE24b peptide and the LRR domain of TaCLV1 (TaCLV1-LRR). GST-tagged TaCLV1-LRR peptides were labeled with fluorescent NT647. The C-terminally encoded peptide 5 (TaCEP5) was used as negative control. The dissociation constant (K_d) was as indicated. ΔFNorm[‰]: change in normalized fluorescence. Central values and error bars represent mean ± s.d. ($n = 3$

biologically independent experiments). **d** *TaCLV1* knockout mutants show decreased density of lateral root and lateral root primordium compared to the control. Scale bar, 5 cm. Phenotyping was performed using 9 day-old seedlings of *TaCLV1* knockout lines (*Taclv1cr-12* and *Taclv1cr-15*) and wild type (Fielder) cultured in Hoagland medium. The box plots display the interquartile range, comprising the first quartile, median, and third quartile, while the whiskers extend from the minimum to the maximum values. Two-tailed Student's *t*-test, ($n = 30$). **e** Comparison of lateral root density and lateral root primordium density of 9 day-old seedlings between *TaCLV1* knockout mutants (*Taclv1cr-12* and *Taclv1cr-15*) and wild type (Fielder) in response to TaCLE24b peptide application. The box plots display the interquartile range, comprising the first quartile, median, and third quartile, while the whiskers extend from the minimum to the maximum values. Two-tailed Student's *t*-test, ($n = 30$).

treatment. Although both NIL-E and NIL-K lines exhibited increased lateral root density under peptide conditions, however, the NIL-K lines showed decreased responses compared to NIL-E, as the average density of LPRs plus LRs increased from 1.428 to 2.061 for NIL-E (44.3% increase), but from 0.976 to 1.316 for NIL-K (34.8% increase; Supplementary Fig. 3c). Furthermore, we generated knockout mutants with loss-of-function of A-, B- and D-homolog of *TaSG-D1* (*Tasg-d1cr-6* and *Tasg-d1cr-9*), which showed 54.2% and 44.4% increases in ELR density, respectively, compared to the control (average of 1.416 and 1.326 vs. 0.918 for WT [Fielder]), as well as ~66.6% and ~52.2% increases of DLRP density, respectively, compared to the WT (average of 1.696 and 1.549 vs. 1.018 for WT [Fielder]; Fig. 3c, d and Supplementary Fig. 3d). Moreover, the *TaSG-D1* loss-of-function mutants showed almost complete insensitivity to TaCLE24b peptide treatment (Fig. 3e). Thus, the results collectively suggest that *TaSG-D1* functions downstream of TaCLE24b, and is a negative regulator of primordium formation and lateral root outgrowth in wheat.

Further analysis revealed that TaCLV1 interacts with TaSG-D1, as evidenced by pull-down, split-luciferase complementation imaging (split-LUC), co-immunoprecipitation (Co-IP) and yeast two-hybrid assay (Y2H) assays (Fig. 3f–i). This interaction leads to phosphorylation and consequently degradation of TaSG-D1 according to phos-tag mobility shift assay and protein degradation analysis, whereas the proteasome inhibitor MG132 impeded the TaCLV1-mediated degradation of TaSG-D1 (Fig. 4a–c). Furthermore, split-LUC assays showed that TaCLV1 exhibited a stronger interaction with TaSG-D1 than TaSG-D1^{E286K} (Supplementary Fig. 4a). In addition, cell-free assays showed

that a faster degradation rate of TaSG-D1 mediated by TaCLV1 in comparison to TaSG-D1^{E286K} (Supplementary Fig. 4b). Moreover, TaCLE24b peptide enhances the binding affinity between TaCLV1 and TaSG-D1 (Supplementary Fig. 5a, b), improving TaCLV1-mediated phosphorylation of TaSG-D1, and thereby promoting its degradation rate and alleviating its repression effects on lateral root development (Supplementary Fig. 5c, d and Fig. 4d). This regulation module positively fine-tunes lateral root development (Fig. 4e).

To investigate the genetic relationship between *TaCLV1* and *TaSG-D1*, we performed manual hybridization to produce F1 seeds by crossing the *Tasg-d1* triple mutant with the heterozygous *Taclv1* triple mutant. As controls, we also generated F1 seeds by crossing *Tasg-d1* with the wild type (Fielder), and *Taclv1* with the Fielder, respectively (Methods). The F1 seedlings from *Tasg-d1×Taclv1* exhibited a significant enhancement in ELR and DLRP density, with ~52.9% (average of 1.211 vs. 0.792) and ~91.1% (average of 1.091 vs. 0.571) increases compared to the *Taclv1×Fielder* (Supplementary Fig. 6). Additionally, *Tasg-d1×Taclv1* F1 seedlings showed similar phenotypes to *Tasg-d1×Fielder* seedlings in terms of ELR and DLRP density (Supplementary Fig. 6). Moreover, the combined density of ELR and DLRP in F1 seedlings from *Tasg-d1×Fielder* was notably reduced compared to that of *Tasg-d1* self-hybridization seedlings, whereas *Taclv1×Fielder* exhibited an obviously higher density than that of *Taclv1* self-hybridization, indicating that hybrids with loss function of one parental allele of *TaCLV1* or *TaSG-D1* can lead to phenotypic variations in lateral root development. Together, these lines of evidences suggest that *TaSG-D1* functions downstream of *TaCLV1*.
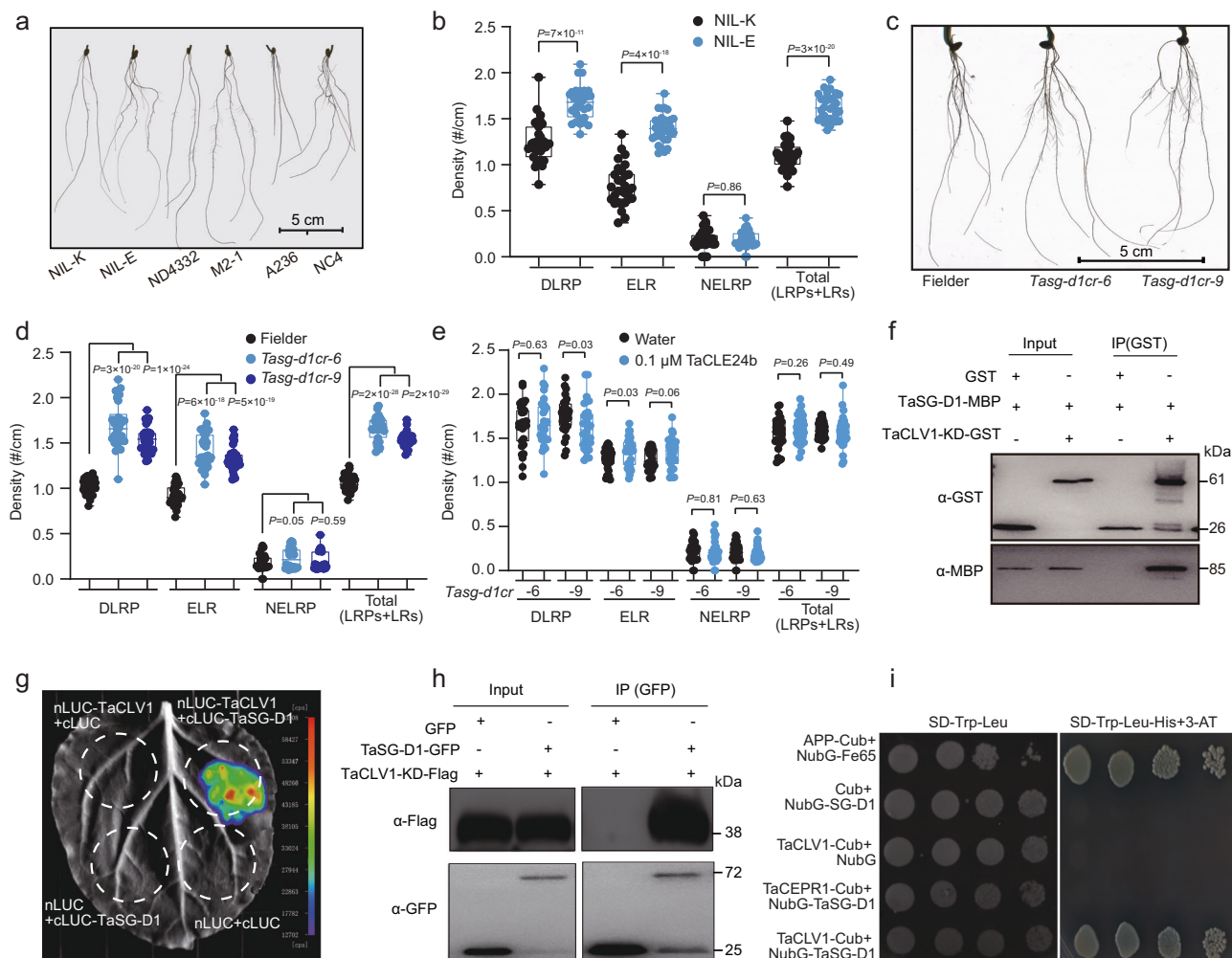
Fig. 3 | TaSG-D1 affects lateral root development via interacting with TaCLV1 in wheat. a Phenotypic analysis of lateral root density and lateral root primordium density of 9 day-old seedlings for the *TaSG-D1/TaSG-D1^E286K* near isogenic lines, the EMS-induced *TaSG-D1^E286K* mutant, and the *TaSG-A1* gain-of-function mutant together with their respective controls. NIL-K, near isogenic line with *TaSG-D1^E286K* (gain-of-function of *TaSG-D1*); NIL-E, near isogenic line with *TaSG-D1*; M2-1, EMS-induced mutant of *TaSG-D1^E286K* in the ND4332 background; A236, gain-of-function of *TaSG-A1* in the NC4 background. Scale bars, 5 cm. **b** Statistical analysis of lateral root density and lateral root primordium density of *TaSG-D1/TaSG-D1^E286K* near isogenic lines. NIL-K, near isogenic line with *TaSG-D1^E286K* (gain-of-function of *TaSG-D1*); NIL-E, near isogenic line with *TaSG-D1*; The box plots display the interquartile range, comprising the first quartile, median, and third quartile, while the whiskers extend from the minimum to the maximum values. Two-tailed Student's *t*-test, (*n* = 30). **c** Phenotypic analysis of lateral root density and lateral root primordium density of 9 day-old seedlings between the *TaSG-D1* knockout mutants (*Tasg-d1cr-6* and *Tasg-d1cr-9*) and controls (Fielder). Scale bars, 5 cm. **d** Statistical analysis of lateral root density and lateral root primordium density of 9 day-old seedlings between the *TaSG-D1* knockout mutants (*Tasg-d1cr-6* and *Tasg-d1cr-9*) and controls (Fielder). The box plots display the interquartile range, comprising the first quartile, median, and third quartile, while the whiskers extend from the minimum to the maximum values. Two-tailed Student's *t*-test, (*n* = 30). **e** Statistical analysis of lateral root density and lateral root primordium density of 9 day-old seedlings

between the *TaSG-D1* knockout mutants (*Tasg-d1cr-6* and *Tasg-d1cr-9*) and wild type (Fielder) in response to TaCLE24b peptide application. The box plots display the interquartile range, comprising the first quartile, median, and third quartile, while the whiskers extend from the minimum to the maximum values. Two-tailed Student's *t*-test, (*n* = 30). **f** Pull-down assay shows the interaction between TaSG-D1 and the kinase domain (KD) of TaCLV1. TaSG-D1-MBP and TaCLV1-KD-GST/GST proteins were incubated with glutathione agarose, and the immunoblotting proteins were detected with anti-MBP and anti-GST antibody. (*n* = 3 biologically independent experiments). **g** Split-LUC assay shows the interaction between TaSG-D1 and TaCLV1. Luciferase activity was determined 48 h after infiltration. **h** Co-IP analysis shows the interaction between TaSG-D1 and the kinase domain (KD) of TaCLV1 in *N. benthamiana* leaves. Immunoblotting was conducted using anti-Flag and anti-GFP antibodies. Immunoprecipitation was performed using anti-GFP magnetic beads. (*n* = 3 biologically independent experiments). (**i**) Yeast two-hybrid assay shows that TaCLV1 interacts with TaSG-D1. TaCLV1 and TaCEPR1 (C-terminally encoded peptide receptor 1) were cloned into pBT3-STE to generate TaCLV1-Cub and TaCEPR1-Cub, respectively. TaCEPR1-Cub was used as negative control. whereas TaSG-D1 was inserted into pPR3-N to produce NubG-TaSG-D1. The transformants were grown on SD-Leu-Trp and SD-Leu-Trp-His plates containing 50 mM 3-AT. The co-transformation of APP-Cub and NubG-Fe65 was used as positive control.

TaCLE24b overexpression improves drought tolerance in plants

Based on our RT-qPCR analysis, we observed that *TaCLE24b* expression is induced by drought stress in root, reaches a peak at 3 h and then decreases (Supplementary Fig. 7). Since lateral root development is closely associated with the response to water deficit[1], we hypothesized that TaCLE24b may play a role in regulating drought tolerance in

plants. To investigate this hypothesis further, we performed RNA-seq analysis and found 5481 differentially expressed genes (4659 upregulated and 822 downregulated) in *TaCLE24* knockout lines and 5159 differentially expressed genes (2739 upregulated and 2420 downregulated) in *TaCLE24b* overexpression lines compared to the respective WT. Gene ontology (GO) enrichment analysis showed that
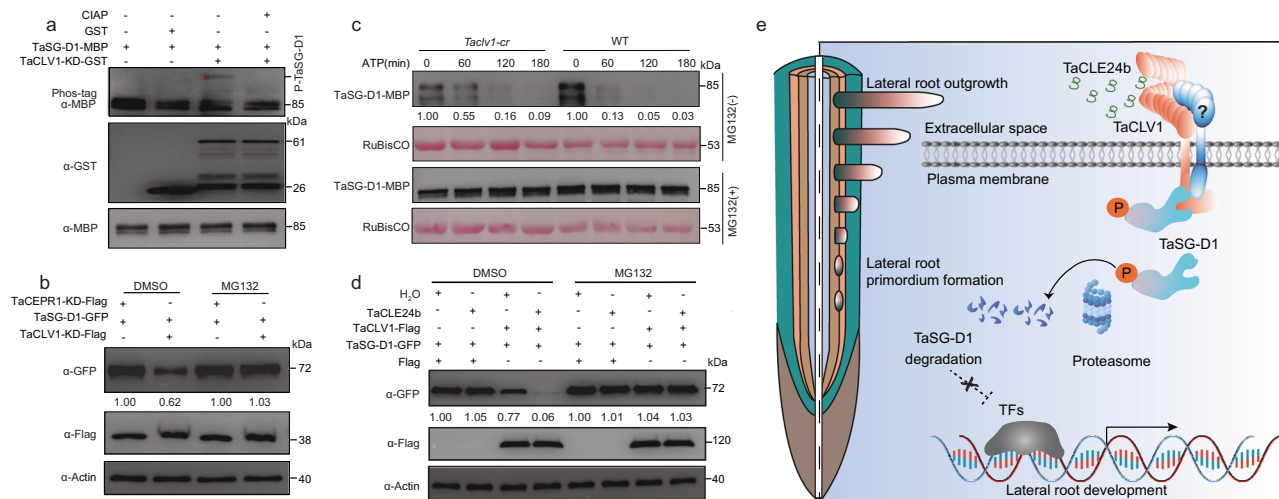
Fig. 4 | TaCLV1 interacts with, and phosphorylates TaSG-D1. a Phos-tag assay shows the kinase domain (KD) of TaCLV1-mediated phosphorylation of TaSG-D1. The phosphorylation status of TaSG-D1 was examined in a phos-tag gel assay (anti-MBP). The levels of TaCLV1 (anti-GST) and TaSG-D1 (anti-MBP) proteins are shown in the SDS-PAGE gel. Phosphorylated TaSG-D1 band is indicated by arrow and red asterisks. ($n = 3$ biologically independent experiments). **b** TaCLV1 reduces TaSG-D1 stability in *N. benthamiana* leaves. TaSG-D1 abundance was examined with anti-GFP antibody. The kinase domain (KD) of TaCLV1 and TaCEPR1 were detected with anti-Flag antibody. Actin was detected with anti-β-Actin antibody as a loading control. TaCEPR1-KD was used as negative control. The relative abundance of TaSG-D1 was quantified using ImageJ software. ($n = 3$ biologically independent experiments). **c** TaCLV1 promotes TaSG-D1 degradation in a cell-free degradation assay. TaSG-D1 abundance was examined with anti-MBP antibody. RuBisCO was detected by Ponceau S staining as a loading control. The relative protein abundance of TaSG-D1

was quantified using ImageJ software. The relative protein level of TaSG-D1 at 0 min was defined as 1.00. ($n = 3$ biologically independent experiments). **d** TaCLE24b accelerates TaSG-D1 degradation. TaSG-D1 was detected with anti-GFP antibody. The full-length cDNA sequence of TaCLV1 was detected with anti-Flag antibody. Actin was detected with anti-β-Actin antibody as a loading control. The relative abundance of TaSG-D1 was quantified using ImageJ software. The relative protein levels of TaSG-D1 without TaCLV1 and TaCLE24b were defined as 1.00. TaCLE24b: synthetic TaCLE24b peptides ($0.1\,\mu M$). ($n = 3$ biologically independent experiments). **e** A working model for the role of the TaCLE24b–TaCLV1–TaSG-D1 signaling pathway during lateral root development in wheat. In the presence of TaCLE24b peptide, TaCLE24b enhances the interaction between TaCLV1 and TaSG-D1, leading to increased phosphorylation and degradation of TaSG-D1, and consequently results in an increase in the density of lateral root and lateral root primordium.

---

the downregulated genes in the knockout lines and the upregulated genes in the overexpression lines are highly enriched in the "response to stress" category (GO:0006950, FDR, 1.4e−07 and 7.9e−20, respectively).

Indeed, *TaCLE24* knockout mutants showed reduced drought tolerance in terms of seedling survival rates under water deficient conditions, with 19.7% [*Tacle24cr-3*] and 23.9% [*Tacle24cr-6*] compared to 100% [WT, Fielder], respectively (Supplementary Fig. 8a, b). Similarly, knockout of *TaCLV1* also resulted in decreased seedling survival rate in response to drought tolerance, with 31.6% [*Taclv1cr-12*] and 35.9% [*Taclv1cr-15*] compared to 94.0% [WT, Fielder], respectively (Supplementary Fig. 8c, d). Whereas *TaCLE24b* overexpression lines showed increased seedling survival rates under water deficient conditions, with 47.2% [*TaCLE24bOE-2*] and 50.0% [*TaCLE24bOE-3*] compared to 8.3% [WT, CB037] (Fig. 5a). In addition, *TaCLE24b* overexpression lines showed increases in the chlorophyll content of flag leaves (average of 35.75 [*TaCLE24bOE-2*] and 36.96 [*TaCLE24bOE-3*] vs. 24.61 [WT]) and thousand kernel weight (average of 38.74 g [*TaCLE24bOE-2*] and 39.75 g [*TaCLE24bOE-3*] vs. 34.49 g [WT]) at the adult stage under drought stress conditions but not under normal conditions (Fig. 5b, c and Supplementary Fig. 9).

We observed that *TaCLE24b* overexpression lines showed reduced water loss (Fig. 5d), and consistently, further investigation revealed that *TaCLE24b* overexpression resulted in an increased proportion of stomata exhibiting closure status compared to the WT under water deficit conditions (average of 68.5% [*TaCLE24bOE-2*] and 73.0% [*TaCLE24bOE-3*] vs. 55.5% [WT, CB037]), but not under normal conditions (average of 41.0% [*TaCLE24bOE-2*] and 41.5% [*TaCLE24bOE-3*] vs. 40% [WT]) (Fig. 5e, f). Whereas *TaCLE24* mutant lines exhibited decreased proportion of stomata exhibiting closure status compared to the WT under water deficit conditions (average of 74.5% [*Tacle24cr-3*] and 73.5% [*Tacle24cr-6*] vs. 85.0% [WT, Fielder]), but not under

normal conditions (average of 38.0% [*Tacle24cr-3*] and 39.0% [*Tacle24cr-6*] vs. 36.5% [WT, Fielder]) (Fig. 5g, h). Interestingly, overexpressing *TaCLE24b* also enhanced drought tolerance in Arabidopsis (Supplementary Fig. 10). These findings collectively suggest that both enhanced lateral root development and increased stomatal closure ratio might contribute to improved drought stress tolerance in *TaCLE24b* overexpression lines.

In summary, our study proposes a model for how the TaCLE24b peptide signaling regulates lateral root development in wheat. TaCLE24b binds to the TaCLV1 receptor, and enhances its binding affinity to TaSG-D1, leading to increased phosphorylation and degradation of TaSG-D1, and consequently results in promoted lateral root and lateral root primordium development. Meanwhile, loss function of *TaCLE24* leads to decreased drought stress tolerance in wheat, whereas constitutive expression of *TaCLE24b* results in enhanced drought stress tolerance probably via comprehensively regulating lateral root development, stomatal closure and chlorophyll content under drought stress conditions. Our findings shed light on the insights into the molecular mechanisms underlying lateral root development and provide new gene resources for the drought stress tolerance improvement in plants (Fig. 4e).

Methods

Plant materials and growth conditions

Spring wheat cultivar 'CB037' and 'Fielder' (*Triticum aestivum* L.) were used for gene cloning, expression analyses, and genetic transformation. The seeds were surface-sterilized with 1% sodium hypochlorite for 15 min and rinsed with distilled water. The sterilized seeds were then soaked overnight in distilled water at room temperature in the dark. Germinated seeds were planted in soil in greenhouse at a relative humidity of 60% and 25/20 °C (day/night) temperatures, with a light intensity of 3000 lux (Master
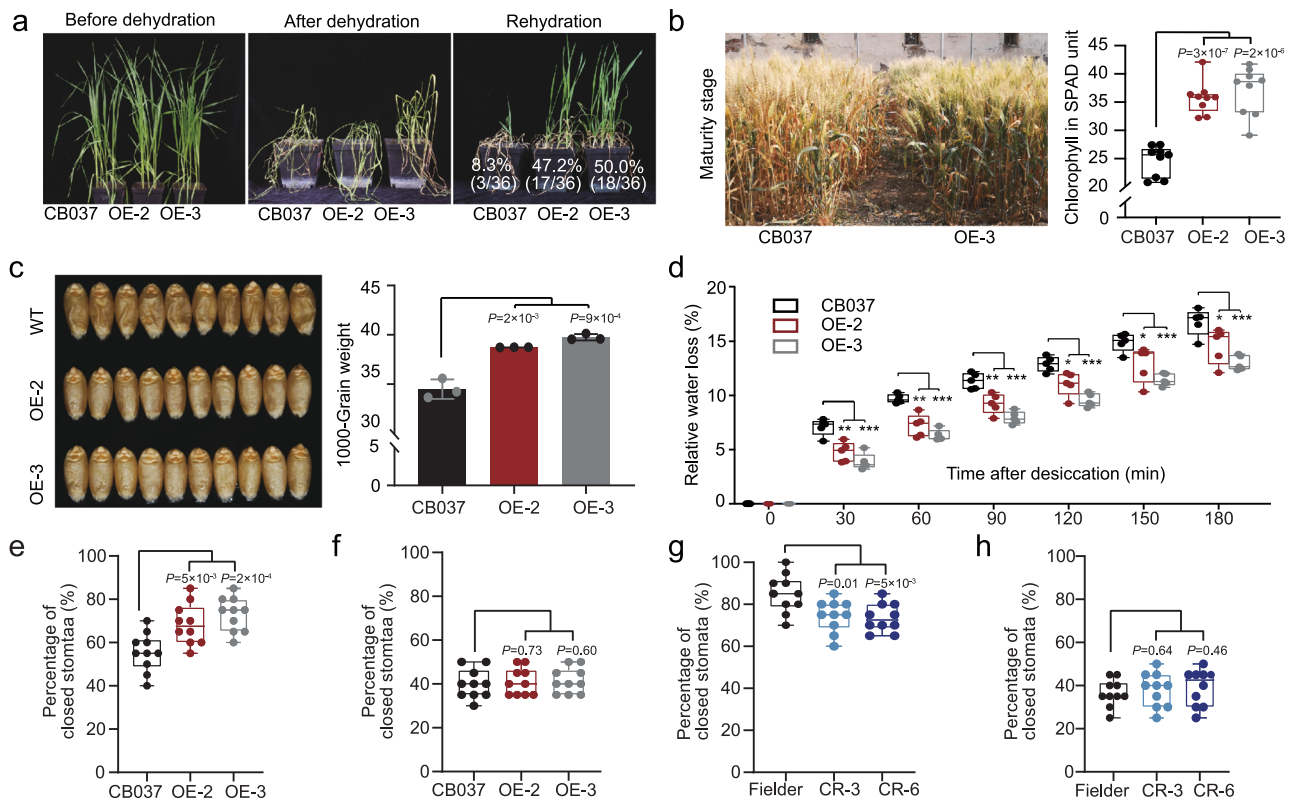
Fig. 5 | Constitutive expression of *TaCLE24b* contributes to drought stress tolerance in wheat. a *TaCLE24b* overexpression lines exhibit enhanced drought tolerance compared to the wild type (CB037). 10 day-old seedlings were subjected to drought stress for 14 days and rehydrated for 10 days before phenotyping. The percentage represents the seedling survival rate. ($n = 3$, twelve seedlings were used for calculation of percentage for each replication). **b** Phenotyping of *TaCLE24b* overexpression lines and WT at maturity under drought stress conditions (left). Flag leaf chlorophyll contents of *TaCLE24b* overexpression lines and WT at maturity under drought stress conditions (right). The box plots display the interquartile range, comprising the first quartile, median, and third quartile, while the whiskers extend from the minimum to the maximum values. Two-tailed Student's *t*-test, ($n = 9$). **c** Seed phenotypes and thousand-kernel weight of WT and *TaCLE24b* overexpression lines under drought stress conditions. Error bars represent standard deviation. Two-tailed Student's *t*-test, ($n = 3$, 200 seeds were used for calculation of thousand-kernel weight for each replication). **d** *TaCLE24b* overexpression lines show reduced water loss compared to the wild type. Leaves of 14 day-old plants were detached and weighed at 30 min intervals. The box plots display the interquartile range, comprising the first quartile, median, and third quartile, while the whiskers extend from the minimum to the maximum values. * $P < 0.05$, ** $P < 0.01$, *** $P < 0.001$, two-tailed Student's *t*-test, ($n = 5$). **e** Statistical analysis of closed stomata under drought conditions between *TaCLE24b* overexpression lines and WT. The box plots display the interquartile range, comprising the first quartile, median, and third quartile, while the whiskers extend from the minimum to the maximum values. Two-tailed Student's *t*-test, ($n = 10$, 20 stomata were used for calculation of percentage for each replication). **f** Statistical analysis of closed stomata under normal conditions between *TaCLE24b* overexpression lines and WT. The box plots display the interquartile range, comprising the first quartile, median, and third quartile, while the whiskers extend from the minimum to the maximum values. Two-tailed Student's *t*-test, ($n = 10$, 20 stomata were used for calculation of percentage for each replication). **g** Statistical analysis of closed stomata under drought conditions between *TaCLE24* knockout lines and WT. The box plots display the interquartile range, comprising the first quartile, median, and third quartile, while the whiskers extend from the minimum to the maximum values. Two-tailed Student's *t*-test, ($n = 10$, 20 stomata were used for calculation of percentage for each replication). **h** Statistical analysis of closed stomata under normal conditions between *TaCLE24* knockout lines and WT. The box plots display the interquartile range, comprising the first quartile, median, and third quartile, while the whiskers extend from the minimum to the maximum values. Two-tailed Student's *t*-test, ($n = 10$, 20 stomata were used for calculation of percentage for each replication).

GreenPower CG T 400 W E40; Philips). For gene cloning and expression analysis, tissues were harvested from greenhouse-grown plants. All samples were immediately frozen in liquid nitrogen and stored at -80 °C.

Arabidopsis thaliana and *Nicotiana benthamiana* plants were planted in the growth chamber with a relative humidity of 55% and temperature condition of 22/20 °C (day/night). Ecotype Col-0 was used for transgenic plants, *35S:GFP*, *35S:TaCLE24b-GFP* and *35S:TaCLE24b* expression cassettes were transformed into Arabidopsis by *Agrobacterium tumefaciens*-mediated floral dip method. *N. benthamiana* transgenic plants for transient expression analyses were generated by *Agrobacterium tumefaciens*-mediated transformation. The primers used in these experiments are listed in Supplementary Data 1.

Synthetic peptides treatment

According to the AlphaFold 3 modeling structure of the TaCLV1-TaCLE24b complex and previous studies[22–24], we predicted the mature sequence of the TaCLE24b peptide as RLSPGGSNPQHH. The mature TaCLE24b peptide (RLSPGGSNPQHH) was synthesized by Genscript (China) with a purity of >95%. The peptides were dissolved in deionized water. Wheat seedlings were treated with different concentrations of synthetic TaCLE24b for 9 days. Firstly, measured the length of root branching zone and lateral root formation zone. Subsequently, counted the number of developing lateral root primordium, delayed lateral root primordium and emerged lateral root. The density of lateral root and lateral root primordium were then computed. Imaging was conducted through scanning with an EPSON (Perfection V850

Pro) scanner. Sterile water cultured wheat seedlings were used as control.

Drought stress treatment and phenotypic analysis

(1) Greenhouse-based drought treatment of wheat and Arabidopsis at seedling stage: For wheat, *TaCLE24b* overexpression plants and corresponding WT (CB037) were grown in pots (10 cm × 10 cm × 10 cm) at the growth chamber under 16-h light/8-h dark and 22 °C/20 °C. Twelve plants were planted for each pot, and three replicates were performed with a total of 36 plants. Water concentration was adjusted to 100% at the beginning, and drought stress treatment was applied for 10 day-old seedlings by stopping irrigation for 14 days and then watering was resumed. The *Tacle24* and *Taclv1* knockout lines and the corresponding WT (Fielder) were planted in plastic boxes (8 cm × 8 cm × 8 cm) in greenhouse under 16 h light/8-h dark and 22 °C/20 °C. Nine seedlings were planted for each pot, and thirteen replicates were performed. Water concentration was adjusted to 100% at the beginning, and drought stress treatment was applied for 14 day-old seedlings by stopping irrigation for 14 days, and then watering was resumed. For Arabidopsis, T_3 generation plants were cultivated in pots (5 cm × 5 cm × 5 cm) at the growth chamber. Three independent experiments were performed with a total of 48 Arabidopsis plants. Drought stress treatment was applied by stopping irrigation, and watering was resumed when wilting was observed. All pots were placed randomly and rotation was done every day to minimize the effects of variation in greenhouse climatic conditions.

(2) Field-based drought treatment of wheat at maturity stage: wild-type CB037 and T_4 generation of *TaCLE24b* overexpression lines were grown in blocks containing 10 rows (1.5 m long) at a spacing of 10 cm per pot in a managed environment facility in field. Three replicates for normal and drought treatments were carried out for each genotype plant. For each replicate, 25 seeds per row were sown. A rain-off shelter was built to shield plants from receiving irrigation from rainfall in Qingdao (36°35′N, 120°06′E; 19 m above mean sea level). The tested plants received two irrigations during the grown season (from February 2019 to May 2019), that is, watering after sowing and watering at booting stage. The irrigation was cut off 30 d after the heading period until the wheat was mature. Thousand grain weight was determined using a camera-assisted phenotyping system (Wanshen Detection Technology Co., Ltd, Hangzhou, China). Chlorophyll content was determined using a handhole chlorophyll analyzer SPAD-502 Plus (Henan Chongsheng Instrument Equipment Co., Ltd, Henan, China).

Water loss assay

TaCLE24b overexpression and WT plants were grown in a growth chamber for 14 days with 25/20 °C (day/night) and 60% relative humidity under a 16/8 h light/dark photoperiod. Five leaves were detached, incubated at room temperature and weighed at 30 min intervals. The amount of water loss of wild-type and transgenic plants was calculated by weighing each plant at the times indicated. All changes in fresh weight are presented as percentages.

Measurement of stomatal traits

TaCLE24b overexpression lines and knockout mutant lines as well as their respective controls, CB037 and Fielder, were treated simultaneously with or without drought stress for 12 h. The third leaves were collected from the plants and immersed in Fixative Solution (Alcohol Acetate Formalin, FAA). Abaxial epidermal strips were peeled and mounted on slides. Stomatal imaging was conducted using a Microcamera (LC35 OLYMPUS, Japan) attached to a microscope (CX23 OLYMPUS, Japan).

RNA sequencing and qRT-PCR analysis

For RNA-seq analysis, root of 9 day-old wheat seedlings (Fielder and *Tacle24cr*; CB037 and *TaCLE24bOE*) were used to extract total RNA with TRIzol™ reagent (Thermo Fisher Scientific, Waltham, MA, USA). Strand-specific RNA libraries were constructed and sequenced on a Novaseq 6000 platform by BerryGenomics Biotechnology (Beijing, China). Three biological replicates were performed for each sample. After screening and trimming, the clean reads were mapped to the wheat reference genome (IWGSC RefSeq v1.1), and DESeq2 was used for DEG analysis with an absolute value of $\log_2$ (fold change) ≥ 1 and adjusted $P < 0.05$. GO enrichment analysis was performed using the clusterProfiler R package (https://www.R-project.org/). For quantitative RT-PCR (qRT-PCR) analysis, cDNA was synthesized from the total RNA using HiScript II Q RT SuperMix (Vazyme Biotech, Nanjing, China) as described in the supplier's instructions. The cDNA was diluted and was used as a template for qRT-PCR. qRT-PCR was performed on an optical 96-well plate with a CFX96 Real-Time PCR Detection System (Bio-Rad) using AceQ qPCR SYBR Green Master Mix (Vazyme Biotech). *TaActin* (TraesCS5A02G124300) was used as an internal control for data normalization. The PCR conditions consisted of an initial step at 95 °C for 3 min, followed by 40 cycles of 95 °C for 15 s, 60 °C for 15 s, and 72 °C for 15 s, and a final dissociation stage with the temperature increasing from 65 °C to 95 °C. Relative transcript levels were calculated using the $2^{-\Delta\Delta Ct}$ method[25]. For each sample, PCR amplification was repeated three times, and the average $2^{-\Delta\Delta Ct}$ values were used to determine the differences in gene expression by two-tailed Student's t-test. All primers used for qRT-PCR are listed in Supplementary Data 1.

Identification of candidate TaCLE24b receptor

To identify potential receptor kinases for the TaCLE24b peptide, we initially conducted a blast analysis against the wheat genome using Arabidopsis CLE peptide-related receptors (*CLV1*, *CLV2*, *BAM1*, *BAM2*, *BAM3*, *PXY*, *CRN*, *ACR4* and *RPK2*), resulting in the identification of 61 potential targets. Among these, 20 candidates were clustered together with *CLV1*, *BAM1*, *BAM2*, and *BAM3*, highlighted in orange (Supplementary Fig. 2b). According to the expression profiling data (http://bar.utoronto.ca/efp_wheat/cgi-bin/efpWeb.cgi), we observed that the wheat homologs of *BAM1* (TraesCS2D02G255900, TraesCS2A02G268300, TraesCS2B02G266700) and *BAM2* (TraesCS5A02G407500, TraesCS5B02G412400, TraesCS5D02G417400) exhibit high expression levels in the spike, while the homologs of *BAM3* (TraesCS4A02G224800, TraesCS4B02G091400, TraesCS4D02G235800) and *PXY* (TraesCS7A02G305700, TraesCS7B02G205900, TraesCS7D02G302400) show elevated expression in the shoot. Interestingly, the wheat homologs of *CLV1* (TraesCS7D02G521200, TraesCS7A02G533800 and TraesCS7B02G758300LC) are predominantly expressed in the root, mirroring the expression pattern of *TaCLE24b*. However, TraesCS7A02G533800 lacks a signal peptide, potentially impacting its localization and function, whereas TraesCS7B02G758300LC is a low-confidence gene that may affect its transcription and translation, leading us to select TraesCS7D02G521200 (marked in yellow) for further analysis.

Generation of *TaCLE24b*, *TaCLV1* and *TaSG-D1* transgenic plants

To generate knock-out mutants of *TaCLE24*, *TaCLV1* and *TaSG-D1* via CRISPR/Cas9 method, single guide RNAs (sgRNAs) were designed based on the exon sequence of three genes using the E-CRISP Design website (http://www.e-crisp.org/E-CRISP. html). Two reverse complementary sgRNA sequences with *Bsa*I cohesive ends were synthesized. The MT_1T_2 vector was amplified using two pairs of primers containing the sgRNAs and then cloned into the CRISPR/Cas9 vector pBUE411. To generate *TaCLE24b* overexpression wheat lines, the coding sequences (CDS) of *TaCLE24b* (TraesCS5B02G418500) were amplified and cloned into the entry vector pWMB003 under promoter *Ubi* by using the restriction enzymes *Sma*I and *Sac*I. Finally, the *Ubi* promoter with *TaCLE24b* were cloned into the destination vector pMWB111 by using the restriction enzymes *Hind*III. The recombinant plasmids were

transformed into wheat cultivar Fielder (for knock-out) or CB037 (for overexpression) via *Agrobacterium*-mediated (strain EHA105) transformation[26]. For lateral root phenotyping, uniformly germinated seeds of T_4 generation were cultured in Hoagland's medium for 9 days, and the lateral root (primordium) density was counted before scanning by EPSON scanner (Perfection V850 Pro). The sequences of sgRNAs are listed in Supplementary Data 1.

Generation and phenotypic analysis of F1 seedlings
We performed manual hybridization using the *Tasg-d1* triple mutant (*Tasg-d1cr-9*) and the heterozygous *Taclv1* triple mutant (*Taclv1cr-15*: homozygous mutations in the A- and D- genomes, and heterozygous mutations in the B- genome) to obtain F1 seeds. We only selected F1 seedlings in which all three homeologs (A-, B-, and D-) of *TaCLV1* genes have been edited and heterozygous according to sequencing analysis. As controls, we also generated F1 seeds by crossing *Tasg-d1* with the wild type (Fielder), and *Taclv1* with the Fielder, respectively. Similarly, the F1 seedlings from the *Taclv1*×Fielder, with all three homologous genes (A-, B-, and D-) of *TaCLV1* edited and heterozygous, were retained for further analysis. The density of lateral root and lateral root primordium of 9 day-old F1 seedlings were analyzed. Imaging was conducted through scanning with an EPSON (Perfection V850 Pro) scanner.

GUS histochemical assay
For further analysis, because *TaCLE24b* exhibits high expression level in the root, whereas *TaCLE24a* and *TaCLE24d* are barely expressed in all examined tissues (Supplementary Fig. 1a). The 2-kb sequence upstream of the transcription start site of *TaCLE24b* (TraesCS5B02G418500) was amplified and cloned into the plant GUS reporter expression vector pBGWFS7 (Invitrogen, USA) and transformed into wheat cultivar Fielder. The 7 day-old seedling roots from wheat transgenic lines (Fielder background) were cut, vacuum-infiltrated with staining buffer (2 mM potassium ferricyanide, 10 mM phosphate buffer, 8 mM EDTA, 0.5% Triton X-100 and 1 mg/mL X-Gluc) and subsequently incubated overnight at 37 °C. The tissues were then incubated in ethanol: acetic acid (1:1) for 6 h and washed by 70% ethanol. The samples were detected by light microscopy (SEX16, OLYMPUS, Japan).

In situ hybridization analysis
Seedling roots were fixed with 10% neutral-buffered formalin (NBF) with 50% ethanol solution, embedded in paraffin and sectioned at a thickness of 5 μm. The unique probes of *TaCLE24b* and *TaCLV1* were labeled by using digoxigenin-11-ddUTP (Roche DIG gel shift kit, Basel, Switzerland). Pretreatment of sections, hybridization, and immunological detection were carried out as described previously[27]. The probe sequences used for analysis are listed in Supplementary Data 1.

Protein expression and purification
The protein expression and purification assays were performed as previously described[28]. cDNA sequences encoding the extracellular domains of TaCLV1 (residues 58-668 aa, designed as TaCLV1-LRR), kinase domain of TaCLV1 (residues 725–1050 aa, designed as TaCLV1-KD) and TaSG-D1 were cloned into the pMAL-c5x or pGEX-6P-1 vectors and transformed into *Transetta* (DE3) *E. coli* Chemically Competent Cells (TransGen, Beijing, China). For the expression of MBP-tagged and GST-tagged proteins, induced with 0.2 mM isopropyl-β-D-thiogalactopyranoside (IPTG) for 12 h at 16 °C. The cells were subsequently harvested, washed, and re-suspended in lysis buffer (50 mM Tris-HCl pH 7.5, 100 mM NaCl, 1 mM Na$_2$EDTA, 5% glycerol (v/v), and 1 mM PMSF). The cells were lysed by sonication on ice and centrifuged at 13000 g for 30 min at 4 °C, and the supernatants were incubated with amylose resin (New England Biolabs, UK, E8021L) for MBP fusion proteins and glutathione agarose resin (TransGen Biotech, ProteinIso

GST Resin, DP201-01) for GST fusion proteins. The primers used for vector construction are listed in Supplementary Data 1.

Subcellular localization assay
The full-length open reading frame of *TaCLV1* was amplified and cloned into the pCAMBIA-SUPER1300 (CAMBIA) vectors with a GFP tag at the C-terminus. The fusion construct *p35S:TaCLV1-GFP* and the *p35S:GFP* control were separately infiltrated into *N. benthamiana* leaves by *Agrobacterium* (GV3101)-mediated transient transformation. In one set of *N. benthamiana* leaves, *p35S:PIP2-mCherry* was co-expressed as plasma membrane marker. In another set, *N. benthamiana* leaves were infiltrated with 50 μM FM4-64 dye (CD4673; Coolaber, China) before observation. Subcellular localization of GFP-tagged proteins, mCherry-tagged proteins or FM4-64 was determined using a Zeiss LSM 880 confocal microscope (LSM880; Carl Zeiss, Heidenheim, Germany) 48 h after infiltration. Excitation/emission wavelengths were 488 nm/500-530 nm for GFP, 561 nm/580-620 nm for mCherry and 543 nm/580-650 nm for FM4-64, respectively. The primers used for analysis are listed in Supplementary Data 1.

Split-luciferase complementation assay
To investigate the interaction between proteins, the coding sequences of TaCLV1, TaSG-D1 and TaSG-D1^{E286K} were cloned into n-LUC or c-LUC vectors separately. *Agrobacterium tumefaciens* strain GV3101 cells containing different constructs were mixed prior to infiltration into *N. benthamiana* leaves. At 48 h after infiltration, LUC activity imaging was analyzed by Night SHADE LB 985 (Berthold Technologies, Bad Wildbad, Germany). The primers used for analysis are listed in Supplementary Data 1.

Immunoblot analysis
Protein extracts were separated by 10% (v/v) SDS-PAGE and transferred to a polyvinylidene fluoride membrane (cat.no.162-0177; Bio-Rad) for 60 min at 300 mA under temperature-controlled conditions. The membrane was blocked using 5% (w/v) defatted milk for 1 h and incubated overnight at 4 °C in 1× Tris-buffered saline containing Tween 20 (TBST; 1× TBS with 0.1% [v/v] Tween 20) and antibodies (1:2000). After washing three times with 1 × TBST for 10 min each time, the membrane was incubated in 5% (w/v) defatted milk-1 × TBST solution containing the secondary antibody (1:5000) for 1 h at room temperature, followed by three washes (10 min each time) with 1 × TBST. Finally, the proteins were detected using chemiluminescent HRP substrate (Millipore, USA). The chemiluminescence signals were detected using the ChemiScope 6000 imaging system (Clinx, China).

Co-immunoprecipitation assay
p35S:TaSG-D1-GFP and *p35S:TaCLV1-KD-Flag* as well as *p35S:TaSG-D1-Myc*, *p35S:TaCLV1-GFP* and TaCLE24b peptides (0.1 μM) were transformed into *Agrobacterium tumefaciens* (strain GV3101) and infiltrated into *N. benthamiana* leaves. After 48 h, the injected leaves were detached and homogenized in liquid N$_2$. Total proteins were extracted using lysis buffer (50 mM Tris-HCl pH 7.5, 150 mM NaCl, 5 mM Na$_2$-EDTA pH 8.0, 0.1% NP-40, 1% Triton X-100 [v/v], 0.6 mM PMSF, 20 μM MG132, 1× protease inhibitor cocktail [Roche]) for 30 min at 4 °C, followed by centrifugation at 13000 g for 20 min at 4 °C to remove cellular debris. The supernatants were incubated with paramagnetic anti-GFP microbeads at 4 °C for 2 h. The samples were applied to a magnetic beads separator to collect the beads, which were washed three times with Co-IP buffer. The proteins were eluted from the beads by boiling in elution buffer. The Immunoprecipitated samples were analyzed by immunoblotting with anti-Myc (1:5000 dilution; HT101-01; TransGen Biotech, Beijing, China), anti-GFP (1:5000 dilution; HT801-01; TransGen Biotech, Beijing, China) antibodies

and anti-Actin (1:5000 dilution; CW0264M; CWBIO, China). The primers used for analysis are listed in Supplementary Data 1.

Pull-down assay
TaSG-D1-MBP in combination with GST or TaCLV1-KD-GST proteins, were applied to glutathione agarose resin (TransGen Biotech, ProteinIso GST Resin, DP201-01), and incubated at 4 °C for 2 h with gentle mixing. The bound resins were washed five times with washing buffer containing 50 mM Tris-HCl (pH 7.5), 50 mM NaCl, 0.1% Triton X-100 (v/v) and 1 mM PMSF, and boiled in 2 × SDS loading buffer for 5 min for immunoblot analysis. The proteins eluted from the resins were detected with anti-GST antibody (1:5000 dilution; HT601-01, TransGen, China) and anti-MBP antibody (1:5000 dilution; AE075, ABclonal Technology, China). The primers used for analysis are listed in Supplementary Data 1.

Yeast two-hybrid assay
The split-ubiquitin membrane yeast two-hybrid system was used in this study[29]. The yeast two-hybrid assays were performed according to the manufacturer's protocol of the DUAL membrane kit 3. The full-length TaCLV1/TaCEPR1 coding sequence was separately cloned into the pBT3-STE vector, while the full-length TaSG-D1 coding sequence was cloned into pPR3-N. The constructs and their vector controls were co-transformed into the NMY51 strain. The colonies grown on synthetic defined (SD) medium without Leu and Trp were transferred onto SD/-Leu-Trp-His selection medium with 50 mM 3-amino-1,2,4-triazole (3-AT) to confirm the protein–protein interaction. The primers used for analysis are listed in Supplementary Data 1.

Microscale thermophoresis assay (MST)
To test the binding affinity of TaCLE24b peptides with the TaCLV1, MST assay was conducted by using Monolith NT.115 (NanoTemper Technologies). Firstly, 10 μM purified TaCLV1-LRR-GST proteins were fluorescently labeled using a MO-L001 Monolith™ Protein Labelling Kit RED-NHS 2nd generation (MO-L001, NanoTemper, Germany) following the manufacturer's instructions. Next, the labeled TaCLV1-LRR-GST (2 μM) proteins were incubated with varying concentrations of chemical synthesized TaCLE24b/TaCEP5 peptides in buffer (137 mM NaCl, 2.7 mM KCl, 10 mM Na_2HPO_4, 2 mM KH_2PO_4, 0.05% Tween 20). Finally, the samples were loaded into silica capillaries (Monolith™ NT.115 Standard Treated Capillaries, MO-K002) and measured by using Monolish NT.115 (NanoTemper Technologies) at 23 °C, medium MST power, 20% LED power. The data were further analyzed by MO. Affinity Analysis software (V2.3*).

In vitro phosphorylation assay
In vitro phosphorylation assays were performed as previously described with minor modifications[30,31]. MBP-tagged TaSG-D1 protein and GST-tagged TaCLV1-KD proteins were co-incubated in a total volume of 20 μl of kinase reaction buffer (20 mM Tris-HCl [pH 7.5], 5 mM $MgCl_2$, 0.1 mM $CaCl_2$, 50 μM ATP, and 2 mM DTT) at 30°C for 30 min. The reaction was stopped by adding 5 × SDS sample buffer. After boiling at 95°C for 5 min, proteins were separated on SDS-PAGE gels followed immunoblot analysis using anti-MBP antibody (1:5000 dilution; AE075, ABclonal Technology, China), or anti-GST antibody (1:5000 dilution; HT601-01, TransGen, China).

In vivo phosphorylation assay
The constructs of 35S:TaSG-D1-Myc, 35S:TaCLV1-Flag and TaCLE24b/TaCEP5 peptides (0.1 μM) were transformed into Agrobacterium tumefaciens strain GV3101 separately. Various blends of plasmids were co-expressed into 4 week-old N. benthamiana leaves. After 48 h, the infiltrated N.benthamiana leaves were detached and homogenized in liquid N_2. Next, total proteins were extracted using 2 × protein loading buffer and boiled for 10 min. The Immunoprecipitated samples were analyzed by immunoblotting with anti-Flag (1:5000 dilution; SAB4301135; Sigma, USA), anti-Myc (1:5000 dilution; HT101-01; TransGen Biotech, Beijing, China) and anti-Actin (1:5000 dilution; CW0264M; CWBIO, China).

Phos-tag mobility shift assay
The Phos-tag SDS-PAGE were prepared according to the manufacturer's guidebook (Wako Chemicals, USA, 304-9352). Phosphorylated proteins from the phosphorylation assays were separated on 10% SDS-PAGE gels with 50 μM Phos-tag and 100 μM $MnCl_2$ followed immunoblot analysis using anti-MBP antibody (1:5000 dilution; AE075, ABclonal Technology, China).

Cell-free protein degradation assay
To investigate the degradation of TaSG-D1 and TaSG-D1^{E286K} in vitro, we carried out cell-free protein degradation experiment as described previously with minor modifications[32]. Briefly, total proteins of WT, TaCLV1 knockout lines and TaCLE24b overexpression lines were extracted in buffer containing 50 mM Tris-HCl (pH 8.0), 500 mM sucrose, 1 mM $MgCl_2$, 10 mM EDTA (pH 8.0), 1 mM DTT and 10 mM ATP, respectively. Then the extracted total proteins incubate with purified MBP-TaSG-D1 or MBP-TaSG-D1^{E286K} protein with 50 μM MG132 (133407-82-6, MCE, USA) or DMSO at 30 °C in different time gradients. After incubation, 2 × SDS loading buffer was added to stop the reaction, anti-MBP antibody (1:5000 dilution; AE075, ABclonal Technology, China) was used to detect the TaSG-D1 protein.

In vivo degradation assay
The p35S:TaSG-D1-GFP and p35S:TaCLV1-KD-Flag/TaCEPR1-KD-Flag were transformed into Agrobacterium tumefaciens (strain GV3101) and infiltrated into N. benthamiana leaves in the presence or absence of 50 μM MG132. After 60 h, the injected leaves were detached and homogenized in liquid N_2. The p35S:TaSG-D1-GFP and p35S:TaCLV1-Flag were transformed into Agrobacterium tumefaciens (strain GV3101) and infiltrated into N. benthamiana. After 48 h, the TaCLE24b peptide or H_2O infiltrated the leaves in the presence or absence of 50 μM MG132, after 12 h, the injected leaves were detached and homogenized in liquid N_2. Total proteins were extracted using degradation buffer (20 mM Tris-HCl [pH 7.5], 150 mM NaCl, 1% Triton X-100, 1 mM PMSF, 2 mM DTT, and 2 mM ATP) for 30 min at 4 °C, followed by centrifugation at 13000 g for 20 min at 4 °C to remove cellular debris, 5×SDS buffer was added to stop the reaction. Proteins were separated by 10% SDS-PAGE, anti-Flag (1:5000 dilution; SAB4301135; Sigma, USA) antibodies was used to detect the TaCLV1-KD protein, anti-GFP (1:5000 dilution; HT801-01; TransGen Biotech, Beijing, China) antibodies was used to detect the TaSG-D1 protein.

Statistics and reproducibility
Statistical analysis was performed using GraphPad Prism v.8.0 (GraphPad software). Statistical significance was determined by using unpaired two-tailed Student's t-test for two-group comparisons, and one-way ANOVA for multiple comparisons. Asterisks indicate significant differences (*$P < 0.05$, **$P < 0.01$, ***$P < 0.001$, ****$P < 0.0001$). Different lowercase letters indicate significant differences ($P < 0.05$). All Western Blot experiments were repeated independently three times with consistent results.

Reporting summary
Further information on research design is available in the Nature Portfolio Reporting Summary linked to this article.

Data availability
The RNA-seq data are generated in this study have been deposited in the National Center for Biotechnology Information (https://www.ncbi.nlm.nih.gov/bioproject/PRJNA848851). Source data are provided with this paper.

References

1. Placido, D. F., Sandhu, J., Sato, S. J., Nersesian, N. & Walia, H. J. The LATERAL ROOT DENSITY gene regulates root growth during water stress in wheat. *Plant Biotechnol. J.* **18**, 1955–1968 (2020).
2. Kumar, A., Ram, B. & Raghuwanshi, R. The microbial consortium of indigenous rhizobacteria improving plant health, yield and nutrient content in wheat (*Triticum aestivum*). *Plant Biotechnol. J.* **44**, 1942–1956 (2021). JJoPN.
3. Farooq, M., Hussain, M. & Siddique, K. H. M. Drought stress in wheat during flowering and grain-filling periods. *Crit. Rev. Plant Sci.* **33**, 331–349 (2014).
4. Chen, Y. L., Fan, K. T., Hung, S. C. & Chen, Y.-R. The role of peptides cleaved from protein precursors in eliciting plant stress reactions. *N. Phytol.* **225**, 2267–2282 (2020).
5. Kim, J. S., Jeon, B. W. & Kim, J. Signaling peptides regulating abiotic stress responses in plants. *Front Plant Sci.* **12**, 704490 (2021).
6. Takahashi, F. et al. A small peptide modulates stomatal control via abscisic acid in long-distance signalling. *Nature* **556**, 235–238 (2018).
7. Nakagami, S. et al. CLE3 and its homologs share overlapping functions in the modulation of lateral root formation through CLV1 and BAM1 in *Arabidopsis thaliana*. *Plant J.* **113**, 1176–1191 (2023).
8. Araya, T. et al. CLE-CLAVATA1 peptide-receptor signaling module regulates the expansion of plant root systems in a nitrogen-dependent manner. *Proc. Natl Acad. Sci. USA* **111**, 2029–2034 (2014).
9. Cho, H. et al. A secreted peptide acts on BIN2-mediated phosphorylation of ARFs to potentiate auxin response during lateral root development. *Nat. Cell Biol.* **16**, 66–76 (2014).
10. Czyzewicz, N. et al. Antagonistic peptide technology for functional dissection of CLE peptides revisited. *J. Exp. Bot.* **66**, 5367–5374 (2015).
11. De Smet, I. et al. Receptor-like kinase ACR4 restricts formative cell divisions in the *Arabidopsis* root. *Science* **322**, 594–597 (2008).
12. Dong, W., Wang, Y. H. & Takahashi, H. CLE-CLAVATA1 signaling pathway modulates lateral root development under sulfur deficiency. *Plants Basel* **8**, 11 (2019).
13. Zhang, L. H. et al. Control of root stem cell differentiation and lateral root emergence by CLE16/17 peptides in *Arabidopsis*. *Front Plant Sci.* **13**, 13 (2022).
14. Toyokura, K. et al. Lateral inhibition by a peptide hormone-receptor cascade during *Arabidopsis* lateral root founder cell formation. *Dev. Cell* **48**, 64–75 (2019).
15. Li, Liu, Xia, Niu, Sciences ZJIJoM. Identification and functional analysis of the CLAVATA3/EMBRYO SURROUNDING REGION (CLE) gene family in wheat. *Int. J. Mol. Sci.* **20**, 4319 (2019).
16. Dubrovsky, J. G. & Forde, B. G. Quantitative analysis of lateral root development: pitfalls and how to avoid them. *Plant Cell* **24**, 4–14 (2012).
17. Olsson, V. et al. Look closely, the beautiful may be small: precursor-derived peptides in plants. *Annu. Rev. Plant Biol.* **70**, 153–186 (2019).
18. Ou, Y., Kui, H. & Li, J. Receptor-like kinases in root development: current progress and future directions. *Mol. Plant* **14**, 166–185 (2021).
19. Poliushkevich, L. O., Gancheva, M. S., Dodueva, I. E. & Lutova, L. A. Receptors of CLE peptides in plants. *Russ. J. Plant Physiol.* **67**, 1–16 (2020).
20. Cheng, X. J. et al. A single amino acid substitution in STKc_GSK3 kinase conferring semispherical grains and its implications for the origin of *Triticum sphaerococcum*. *Plant Cell* **32**, 923–934 (2020).
21. Cao, J. et al. Natural variation of STKc_GSK3 kinase TaSG-D1 contributes to heat stress tolerance in Indian dwarf wheat. *Nat. Commun.* **15**, 2097 (2024).
22. Abramson, J. et al. Accurate structure prediction of biomolecular interactions with AlphaFold 3. *Nature* **630**, 24 (2024).
23. Kondo, T. et al. A plant peptide encoded by *CLV3* identified by in situ MALDI-TOF MS analysis. *Science* **313**, 845–848 (2006).
24. Sawa, S., Kinoshita, A., Nakanomyo, I. & Fukuda, H. CLV3/ESR-related (CLE) peptides as intercellular signaling molecules in plants. *Chem. Rec.* **6**, 303–310 (2006).
25. Livak, K. J. & Schmittgen, T. D. Analysis of relative gene expression data using real-time quantitative PCR and the 2(-Delta Delta C(T)) method. *Methods* **25**, 402–408 (2013).
26. Ishida Y., Tsunashima M., Hiei Y., Komari T. Wheat (*Triticum aestivum* L.) transformation using immature embryos. In *Agrobacterium Protocols Methods in Molecular Biology* (ed. Wang, K.) 1223 (Springer, 2015).
27. Sang, X. et al. CHIMERIC FLORAL ORGANS1, encoding a monocot-specific MADS box protein, regulates floral organ identity in rice. *Plant Phys.* **160**, 788–807 (2012).
28. Liu, C. et al. Pollen PCP-B peptides unlock a stigma peptide-receptor kinase gating mechanism for pollination. *Science* **372**, 171–175 (2021).
29. Thaminy, S., Miller, J. & Stagljar, I. The split-ubiquitin membrane-based yeast two-hybrid system. *Methods Mol. Biol.* **261**, 297–312 (2004).
30. Han, X. et al. SnRK1 phosphorylates and destabilizes WRKY3 to enhance barley immunity to powdery mildew. *Plant Commun.* **1**, 14 (2020).
31. Shen, Q. et al. Tomato SlSnRK1 protein interacts with and phosphorylates βC1, a pathogenesis protein encoded by a geminivirus β-Satellite. *Plant Physiol.* **157**, 1394–1406 (2011).
32. Osterlund, M. T., Hardtke, C. S., Wei, N. & Deng, X. W. Targeted destabilization of HY5 during light-regulated development of *Arabidopsis*. *Nature* **405**, 462–466 (2000).

Author contributions

M.X. and Q.S. conceived this project. W.Y., M.F., J.C. and G.C. collected tissue samples and performed experiments. W. Y., M.F., K.Y., Y.Z., H.P., Y.Y., Z.H. and Z.N. analyzed data and collected phenotypic data. F.Q., F.T., M.X., Q.S., M.F. and W.Y. wrote the manuscript. All authors read and approved the final manuscript.

Competing interests

A patent application related to this work has been submitted by M.X., M.F., Q.S., Z.N., H.P., Y.Y. and Z.H. The remaining authors declare no competing interests.

Additional information

Supplementary information The online version contains supplementary material available at https://doi.org/10.1038/s41467-025-57291-x.

Correspondence and requests for materials should be addressed to Mingming Xin.

Peer review information *Nature Communications* thanks Rüdiger Simon, and the other, anonymous, reviewer(s) for their contribution to the peer review of this work. A peer review file is available.

Reprints and permissions information is available at http://www.nature.com/reprints

Publisher's note Springer Nature remains neutral with regard to jurisdictional claims in published maps and institutional affiliations.